Sensors and Actuators B 213 (2015) 268–275

Contents lists available at ScienceDirect

Sensors and Actuators B: Chemical

journal homepage: www.elsevier.com/locate/snb

A fluorescence sensor for Zn^{2+} that also acts as a visible sensor for Co^{2+} and Cu^{2+}

Eun Joo Song[a,b], Gyeong Jin Park[a,b], Jae Jun Lee[a,b], Suyeon Lee[c], Insup Noh[c], Youngmee Kim[d], Sung-Jin Kim[d], Cheal Kim[a,b,**], Roger G. Harrison[e,*]

[a] Department of Fine Chemistry, Seoul National University of Science & Technology, Seoul 139-743, Republic of Korea
[b] Department of Interdisciplinary Bio IT Materials, Seoul National University of Science & Technology, Seoul 139-743, Republic of Korea
[c] Department of Chemical Engineering, Seoul National University of Science & Technology, Seoul 139-743, Republic of Korea
[d] Department of Chemistry and Nano Science, Ewha Womans University, Seoul 120-750, Republic of Korea
[e] Department of Chemistry and Biochemistry, Brigham Young University, Provo, UT, USA

ARTICLE INFO

Article history:
Received 12 November 2014
Received in revised form 16 February 2015
Accepted 17 February 2015
Available online 28 February 2015

Keywords:
Zinc fluorescent sensor
Visible cobalt
Copper sensor

ABSTRACT

Monitoring Zn^{2+} levels in biological environments with fluorescent sensors is important. This paper gives the synthesis and properties of a new Zn^{2+} sensor based on quinoline and pyridylaminophenol. The sensor is selective for Zn^{2+} and remains fluorescent when bound to Zn^{2} even in the presence of other metal ions. Along with fluorescing when bound to Zn^{2+}, the sensor becomes colored when Cu^{2+} or Co^{2+} is added to it. These two metal ions result in the sensor becoming yellow. The crystal structure of the Cu–sensor complex shows that all of the sensor's nitrogens are bound to the metal ion. In studies with living cells, the fluorescence intensity of the sensor correlates to the concentration of Zn^{2+}.

1. Introduction

Zinc ions in biological environments do not have a color, are redox inactive, and are magnetically silent. Small molecules that change fluorescence upon binding to Zn^{2+} have proven successful in their ability to monitor Zn^{2+} concentrations and locations in cells and organisms [1]. To perform their function as a Zn^{2+} sensor in biological environments, a sensor must bind Zn^{2+} in preference to other metal ions, be water soluble, and respond to Zn^{2+} with intense fluorescence [2].

Visible sensors are also significant for the detection and quantification of metal ions. Copper is another essential metal in biology. Cobalt, although to a lesser extent, also occurs in organisms. Although Co^{2+} and Cu^{2+} have *d–d* transitions in the visible region, the transitions are weak and render dilute solutions of the metal ions colorless. Along with the few fluorescent sensors for Co [3], there are a few visible sensors as well. The visible sensors for Co are based on compounds with conjugated rings and nanoparticles [4]. Cu has also been detected with visible sensors. These sensors are based on a variety of molecules including dyes [5], guanidine [6], Schiff bases [7], and other molecules [8].

Multifunctional sensors are becoming more important due to one molecule being able to be used for the detection of more than one metal ion [9]. They include transition metal sensors that give a different response for the following pairs: Cr/Al [10] Cr/Fe [11], Mn/Ag [12], Fe^{2+}/Fe^{3+} [13], Fe/Cu [14], Cu/Zn [15], Cu/Hg [16], Zn/Al [17], and Co/Zn [18]. Often the response is either a visible or fluorescence change for both metals, but in a few cases the change is visible form one metal and fluorescence for the other.

In this paper we present the properties of a dual sensor that fluoresces in the presence of Zn^{2+} and changes color in the presence of Co^{2+} and Cu^{2+}. The sensor relies on quinoline as the origin of fluorescence and pyridylaminophenol [19] as the metal ion-binding group. Quinoline-based receptors have proven to be successful Zn^{2+} sensors [20]. When Zn^{2+} binds the sensor, it fluoresces, making for a way to detect Zn^{2+} in an aqueous environment. The fluorescence due to Zn^{2+} is selective for Zn^{2+} and remains even when other metal ions are present. When Co^{2+} binds to the sensor a new visible absorption band grows in, which also remains in the presence of other metal ions. A crystal structure of the Cu–receptor complex shows the Cu^{2+} binding to the nitrogen atoms of the receptor. The results of using the receptor in living cells are presented.

* Corresponding author. Tel.: +1 801 422 8096.
** Corresponding author. Tel.: +82 2 970 6693.
E-mail addresses: chealkim@seoultech.ac.kr (C. Kim), roger_harrison@byu.edu (R.G. Harrison).

http://dx.doi.org/10.1016/j.snb.2015.02.094
0925-4005/

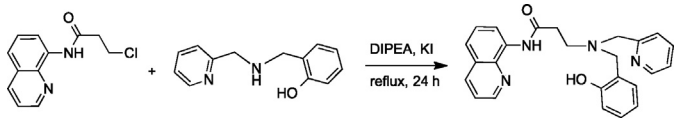

Scheme 1. Receptor synthesis.

2. Results and discussion

The new receptor was synthesized by adding 3-chloro-N-(quinoline-8-yl)propanamide to functionalized amine (Scheme 1). This receptor is similar in structure to receptors with dipicolylamine (dpa) as the binding group, but it differs by having a phenol group in place of a pyridine [21]. The binding to zinc by this receptor should still be strong, even though one oxygen is replacing a nitrogen and a six membered metal–ligand ring will form instead of the five membered metal–ligand ring. This receptor, which has two carbons separating the amine from the phenol, is similar to the sensor that has the same binding domain, but only one carbon between the phenol and the amine [22]. It is expected that this change will result in a weaker binding strength to Zn^{2+} and different binding properties with other metal ions.

The sensor does not fluoresce on its own, however when Zn^{2+} is added to it a fluorescence band at 520 nm grows until one equivalent of Zn^{2+} has been added (Fig. 1). The fluorescence enhancement only occurs with Zn^{2+} ions and does not happen with other metal ions such as Na^{+}, K^{+}, Mg^{2+}, Ca^{2+}, Al^{3+}, Ga^{3+}, In^{3+}, Mn^{2+}, Fe^{3+}, Co^{2+}, Ni^{2+}, Cu^{2+}, Cd^{2+}, and Hg^{2+} (Fig. 2). This fluorescence response to only Zn^{2+} in aqueous solution will serve to allow Zn^{2+} sensing under biological conditions. The binding of Zn^{2+} stops the amide lone pair of electrons from quenching the fluorescence of the quinoline, but unlike with the other transition metals, which also bind to the amide electrons, Zn^{2+} does not quench the fluorescence. This unique property of Zn^{2+} results in the receptor fluorescing with Zn^{2+} and not with other metal ions. The fluorescence due to Zn^{2+} is maintained for hours and is above fifty percent of its original value after 24 h (ESM). The selectivity for Zn^{2+} matches what has been observed for several other receptors [20].

Not only is fluorescence only seen with Zn^{2+}, it is resistant to change by other metal ions. The fluorescence due to the Zn–receptor complex persisted when many other metal ions were added to the complex (Fig. 3). Cu^{2+} and to a smaller extent for Co^{2+} resulted in a decrease in fluorescence intensity. This implies the binding constant of Zn^{2+} to the receptor is stronger than that of many metal ions and comparable to Cu^{2+}. The binding constant for Zn^{2+} was found to be $1.0 \times 10^4\ M^{-1}$ in aqueous-acetonitrile

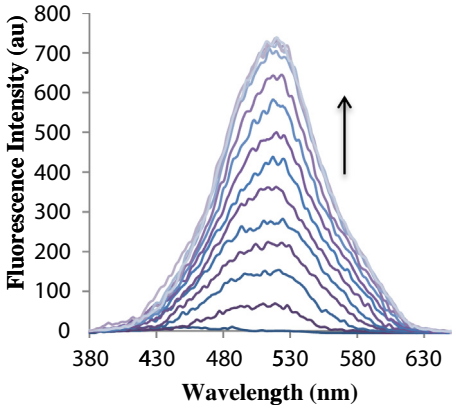

Fig. 1. Fluorescence increase due to Zn^{2+}. (A) Acetonitrile–buffer solution of Zn^{2+} was added in 0.1 equiv. portions to 10 μM receptor in acetonitrile–buffer solution (10 mM HEPES, pH 7.4, 1:1 acetonitrile/buffer, 356 nm excitation).

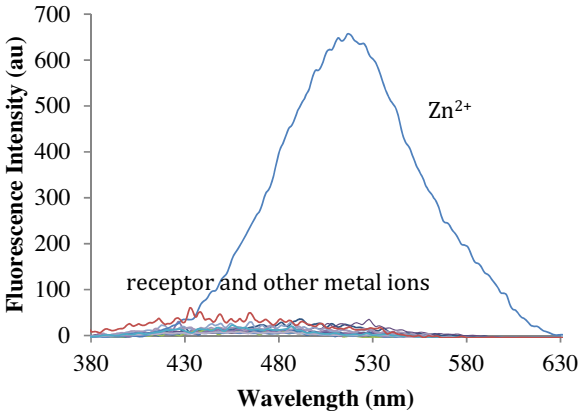

Fig. 2. Receptor fluorescence with metal ions. Zn^{2+} (top spectra) causes fluorescence enhancement, while the receptor shows no fluorescence with other metal ions (spectra near the base line) (10 μM receptor acetonitrile–HEPES buffer solutions, excited at 356 nm).

solutions. This binding constant is similar to what was found for Cu^{2+} ($7.9 \times 10^3\ M^{-1}$) and Co^{2+} ($2.3 \times 10^3\ M^{-1}$) in the same solution. As expected, the binding constant to Zn^{2+} for the receptor was lower than sensors with dipicolylamine, which have binding constants of $4.1 \times 10^{10}\ M^{-1}$ [21]. It is also lower than the binding constant of the sensor with a methylene in place of the ethylene between the phenol and amine, which has a binding constant of $4.0 \times 10^6\ M^{-1}$ [22]. Even with this smaller binding strength, due to the intense fluorescence by the receptor, the Zn^{2+} detection limit of 8.14 nM was found, which concentration is within the range of biological Zn^{2+} concentrations.

The fluorescence due to Zn^{2+} can be turned off and on. When EDTA is added to the Zn^{2+}–receptor complex, the fluorescence is distinguished (Fig. 4). When more Zn^{2+} is added to the solution, fluorescence reappears. Upon the addition of more EDTA, the fluorescence is again stopped. Low pH also causes the fluorescence to be erased. When the pH is below 6, there is not fluorescence, most likely due to the receptor being protonated and not binding to Zn^{2+}. However, when the pH is above 6 and less than 12, fluorescence is strong. The receptor without Zn^{2+} does not fluoresce at any pH. Thus, unlike Zn^{2+} binding, proton binding does not cause fluorescence.

Along with the fluorescent data, absorption changes show a 1:1 binding of Zn^{2+} to receptor. The absorption change of the receptor due to Zn^{2+} binding levels off after one equivalent of Zn^{2+} (Fig. 5). Two absorption bands (245 and 325 nm) decrease and two bands (270 and 375 nm) increase upon Zn^{2+} binding. The 375 nm band tails off into the visible region of light, implying the complex could be exited with visible light. A Job plot also shows 1:1 receptor to Zn^{2+} binding. These absorption changes might be due to

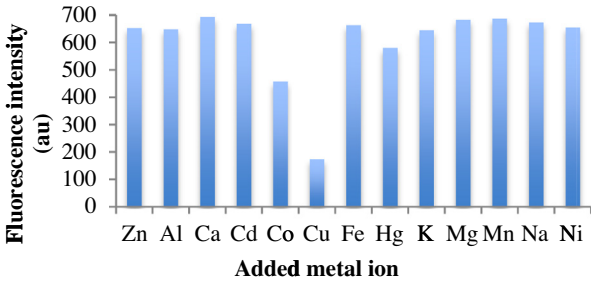

Fig. 3. Fluorescence inhibition by metal ions. The fluorescence (356 nm excitation) of the Zn^{2+}–receptor complex (10 μM acetonitrile–HEPES buffer solution, pH 7.4) remains when most other metal ions (1 equiv.) are added.

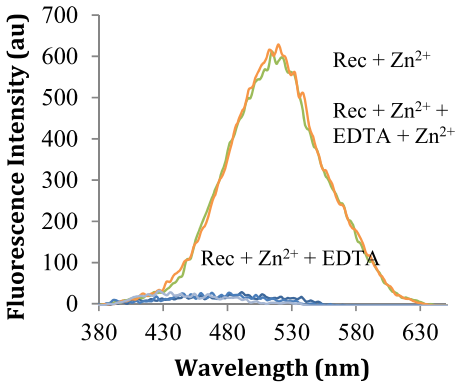

Fig. 4. Fluorescence switching on and off. The fluorescence is lost when EDTA is added (curves along the baseline) and then reoccurs when more Zn^{2+} is added to the solution (curves with fluorescence intensity). A 10 μM receptor acetonitrile–HEPES buffer solution had 1 equiv. of Zn^{2+}, 2 equiv. EDTA, 2 equiv. Zn^{2+} and 2 equiv. EDTA added to it.

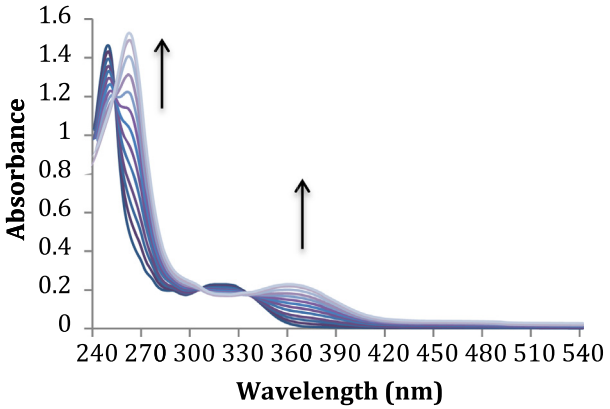

Fig. 5. Absorption change with Zn^{2+} addition. An acetonitrile–HEPES buffer solution of receptor (40 μM) was titrated with an acetonitrile–HEPES buffer solution of Zn^{2+} (0–1.3 equiv.).

deprotonation of the amide nitrogen. Also, mass spectra of the Zn–receptor complex show the dominant species at 475 *m*/*z*, which corresponds to one Zn^{2+} to one receptor.

To learn where the receptor is bonding to the metal ion in the solid-state, crystals of a metal–receptor complex were analyzed. Although the Zn–receptor complex did not crystallize, the Cu–receptor complex did when the receptor was added to $Cu(NO_3)_2$ and NH_4OH in acetonitrile. The receptor formed a 2:2 complex with Cu^{2+} in the solid-state with two Cu–receptor complexes linked by an amide oxygen (Fig. 6). The four nitrogens of the receptor form equatorial planes around copper ions with N—Cu—N bond angles close to 90° and Cu—N bond lengths from 1.95 to 2.05 Å. The axial positions on the coppers are occupied by phenolic oxygens and display the Jahn–Teller effect with elongated Cu—O bonds of 2.42 Å. The amide hydrogens, as well as one phenolic hydrogen have been displaced by the metal ion, resulting in the receptors being anions. The C—O amide bonds are 1.25 Å and shorter than the C—O phenol bonds which are 1.37 Å. The ethyl group between the amine and amide does not deter the receptor binding. Zn^{2+}, which like Cu^{2+} is stable in five and six coordinate environments, is expected to bind in a similar manner to the receptor. Since the

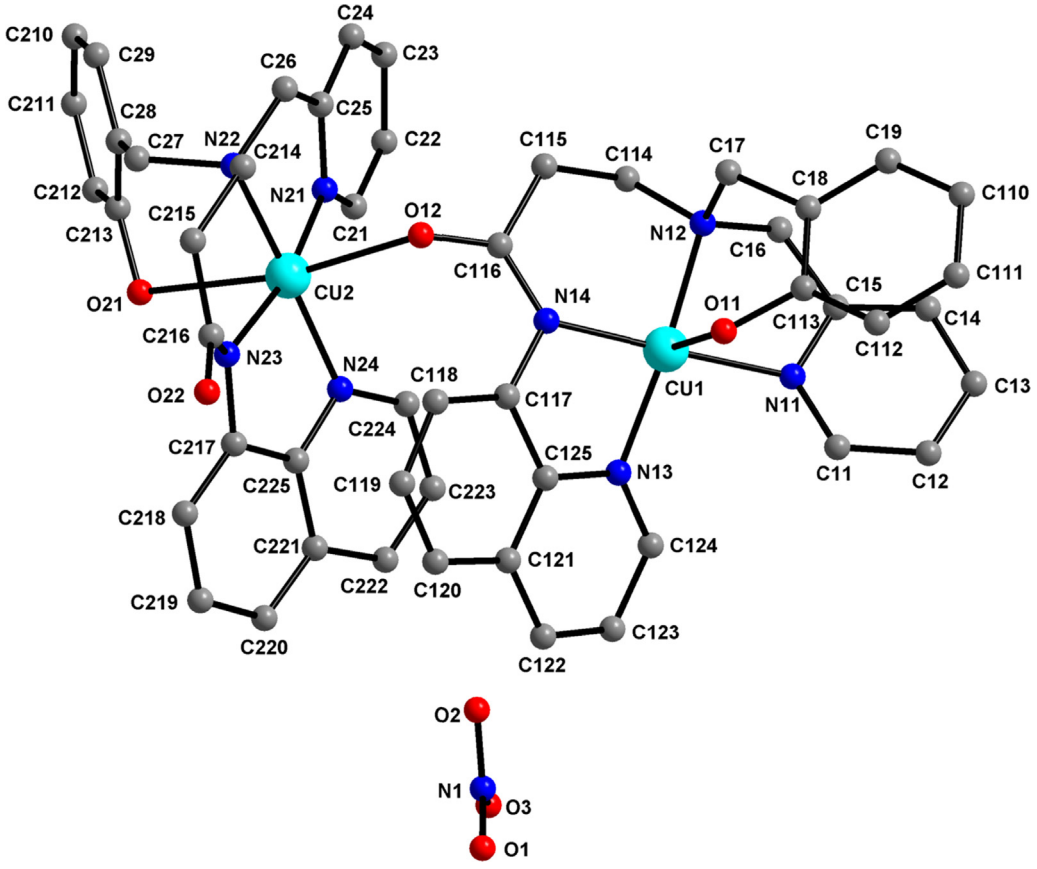

Fig. 6. Crystal structure of the Cu–receptor complex. Two complexes are linked by an amide oxygen. Atom colors: Cu light blue, N dark blue, C gray, O red, and H white. Hydrogen atoms and solvent molecules were omitted for clarity. Selected bond lengths (Å): Cu1-N14 1.954(4), Cu1-N11 1.996(5), Cu1-N13 2.000(4), Cu1-N12 2.019(5), Cu1-O11 2.417(4), Cu2-N24 1.997(4), Cu2-N23 1.997(4), Cu2-N22 2.008(4), Cu2-N21 2.054(4), Cu2-O12 2.352(4), Cu2-O21 2.77(5).

solution data show a 1:1 Cu^{2+} to receptor stoichiometry, we propose the 2:2 complex found the solid state is not stable in solution.

As we were testing the receptor's fluorescence response to Zn^{2+}, we noticed that solutions of the receptor with Cu^{2+} and Co^{2+} became yellow. The receptor's color change was only seen for Cu^{2+} and Co^{2+} and did not correlate to a fluorescence change, which was only observed for Zn^{2+} (Fig. 7). The change in color did correlate to the formation of a new absorption band in the visible region due to these metal ions (ESM). Other metal ions, such as Zn^{2+} and Hg^{2+}, caused the receptor to have a new absorption band, but the band quickly tails off in the visible region and does not result in a color change. As with Zn^{2+}, the receptor binds to Co^{2+} and Cu^{2+} in a one to one ratio as shown by Job plots and mass spectra data.

The color of the Co–receptor complex resists change by other metal ions, it does however, reduce in the presence of Zn^{2+}. Likewise, the color due to the Cu–receptor complex remains constant when most other metal ions are present, but does reduce in intensity when Zn^{2+}, Hg^{2+}, Fe^{3+} and Ni^{2+} are present. The receptor's color change due to Cu^{2+} and Co^{2+} mean small concentrations of these metal ions can be detected. The detection limits for Co^{2+} and Cu^{2+} are 0.85 and 0.98 μM, respectively.

Upon further investigation of the yellow color due to Co^{2+}, it was found that when Co^{2+} is mixed with the receptor under a nitrogen atmosphere, no color is produced. As with Zn^{2+} and Cu^{2+}, cobalt should be bound to the receptor as Co^{2+}. However, with oxygen present, the Co^{2+} might be oxidized to Co^{3+}. It was found that the ^1H NMR signals of the yellow Co–receptor complex were not paramagnetically shifted, which would be the case if Co^{2+} was present. Considering these results leads us to propose that the Co^{2+} is being oxidized to Co^{3+} after binding occurs and the Co^{3+}–receptor complex has a yellow color. It is common for Co^{2+} coordinated to nitrogen ligands to be oxidized by air to Co^{3+}. It should be noted that the color of this complex and the Cu–receptor complex, with their large extension coefficients of $1.1 \times 10^4\ M^{-1}\ cm^{-1}$ and $9.9 \times 10^3\ M^{-1}\ cm^{-1}$ ($\lambda = 375$ nm) respectively, originate from the receptor and are not due to metal ion *d–d* transitions.

Additional evidence of metal binding to the amide group of the receptor was obtained by IR spectra. In an acetonitrile/HEPES buffer solution the receptor has a C=O stretch at 1670 cm^{-1} (ESM). This peak moves to 1631 cm^{-1} when Zn^{2+} is added to the receptor. When Co^{2+} is added to the receptor it moves to 1642 cm^{-1} and when Cu^{2+} is added it moves to 1612 cm^{-1}. Binding of the metal ions results in lower energy C=O frequencies. This can be attributed to the metal cations withdrawing electron density from the amide group and causing it to have less double bond character.

Noting the strong fluorescence response of the receptor for Zn^{2+}, we investigated the ability of the receptor to detect Zn^{2+} in cells. Human dermal fibroblast cells were incubated with 0–200 μM concentrations of $Zn(NO_3)_2$ and after the excess $Zn(NO_3)_2$ was washed off, were incubated with 20 or 30 μM receptor for 30 min at room temperature. Visible images of the cells show healthy cells under all of the Zn^{2+} and receptor concentrations (Fig. 8). The fluorescence images of the cells show that the cells without Zn^{2+} do not fluoresce and increasing concentrations of Zn^{2+} result in increased fluorescence. This shows that original cellular Zn^{2+} is not visible with this receptor, but Zn^{2+} added to the cell is detectable. By plotting the fluorescence as a function of added Zn^{2+}, it is evident that fluorescence increases up to 100 μM of Zn^{2+} (ESM). In combination with Zn^{2+}, the receptor provides distinct images of the cells.

3. Conclusion

A Zn^{2+} sensor based on a quinoxaline chromophore and a phenol–pyridine binding group has been developed and shown to only fluoresce in the presence of Zn^{2+}. The sensor however, shows a visible response to Cu^{2+} and Co^{2+} and becomes yellow in their presence. These metal ions can be detected and distinguished by the naked eye and from other metal ions. When the receptor binds to Cu^{2+}, it uses all of it nitrogen atoms, which atoms form a square planar arrangement. Along with *in situ* fluorescence, the receptor fluoresces in living cells. These studies show that this receptor with its new binding domain containing phenol, provides for weaker Zn^{2+} binding and the possibility of monitoring Zn^{2+} in biological environments. Receptor changes are important to produce different Zn^{2+} fluorophores.

4. Experimental

4.1. Materials and instrumentation

All solvents and reagents (analytical grade and spectroscopic grade) were obtained commercially and used as received. 3-Chloro-N-(quinolin-8-yl)propanamide was prepared as previously reported [22]. NMR spectra were recorded on a Varian 400 spectrometer. Chemical shifts (δ) are reported in ppm, relative to tetramethylsilane $Si(CH_3)_4$. Absorption spectra were recorded at 25 °C using a Perkin Elmer model Lambda 2S UV/Vis spectrometer. The emission spectra were recorded on a Perkin-Elmer LS45 fluorescence spectrometer. Electrospray ionization mass spectra (ESI-MS) were collected on a Thermo Finnigan (San Jose, CA, USA) LCQ™ Advantage MAX quadrupole ion trap instrument. Elemental analysis for carbon, nitrogen, and hydrogen was carried out by using a Flash EA 1112 elemental analyzer (thermo) in Organic Chemistry Research Center of Sogang University, Korea.

4.2. Synthesis of receptor

2-Aminomethyl pyridine (0.62 mL, 6.0 mmol) and 2-hydroxy benzaldehyde (0.54 mL, 5.0 mmol) were dissolved in methanol (15 mL) and stirred for 1 h. Then, $NaBH_4$ (0.1929 g, 5.1 mmol) was added, and the reaction solution was cooled in an ice bath. It was stirred for 2 h and the solvent was removed under reduced pressure to obtain a brown oil. The brown oily residue was dissolved in methylene chloride washed twice with water followed by saturated brine solution. The organic layer was dried over anhydrous Na_2SO_4 and the solvent was evaporated under vacuum. The resultant oil (0.73 g, 3.4 mmol), 3-chloro-N-(quinolin-8-yl)propanamide (0.70 g, 3.0 mmol), N,N-diisopropylethylamine (0.59 mL, 3.2 mmol) and potassium iodide (0.54 g, 3.2 mmol) were dissolved in acetonitrile (30 mL), stirred and refluxed for 1 day under a nitrogen atmosphere. The mixture was cooled to room temperature and the solvent was removed under reduced pressure to obtain a yellow oil, which was purified by silica gel column chromatography (90:1 v/v $CHCl_3$—CH_3OH). Yield: 1.03 g (83.3%). ^1H NMR (400 MHz, DMSO-d_6, 25 °C): $\delta = 10.37$ (s, 1H), 10.09 (s, 1H), 8.87 (d, $J = 4$ Hz, 1H), 8.60 (d, 1H), 8.50 (d, $J = 4$ Hz, 1H), 8.39 (d, $J = 8$ Hz, 1H), 7.63 (m, 3H), 7.56 (t, $J = 8$ Hz, 1H), 7.47 (d, $J = 8$ Hz, 1H), 7.23 (t, $J = 10$ Hz, 2H), 7.04 (t, $J = 6$ Hz, 1H), 6.72 (d, $J = 8$ Hz, 1H), 6.66 (t, $J = 7.2$ Hz, 1H), 3.85 (s, 2H), 3.77 (s, 2H), 2.88 (m, 4H) ppm. ^{13}C NMR (400 MHz, DMSO-d_6, 25 °C): $\delta = 170.7$, 158.2, 156.5, 148.7, 138.1, 136.6, 136.5, 134.7, 128.9, 128.1, 127.8, 126.9, 123.3, 123.1, 122.2, 122.0, 121.7, 118.6, 116.7, 115.4, 58.4, 53.5, 49.5, 34.22 ppm. LRMS (ESI): *m/z* calcd for $C_{25}H_{24}N_4O_2 + H^+$: 412.19; found 412.07. Elemental analysis calcd (%) for $C_{25}H_{24}N_4O_2$: C, 72.80; H, 5.86; N, 13.58; found: C, 72.65; H, 5.95; N, 13.75.

4.3. Preparation of Cu^{2+}–receptor crystals

Acetonitrile solutions of $Cu(NO_3)_2$ (0.0125 mmol, 1 mL), receptor (0.0125 mmol, 1 mL) and NH_4OH (0.0125 mmol, 1 mL) were

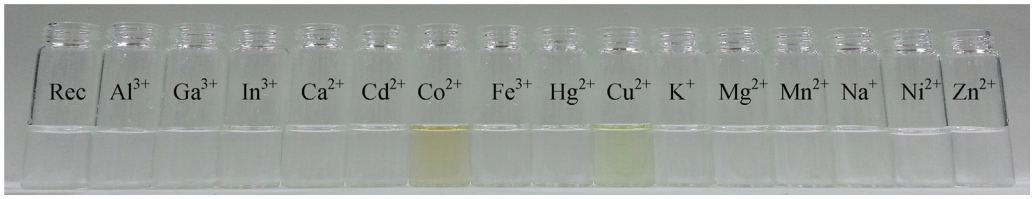

Fig. 7. Visible color of receptor solutions with metal ions. Co^{2+} and Cu^{2+} result in the receptor becoming yellow, while the other metal ions cause no color change. Receptor (50 μM) with 1 equiv. of metal ion is in an acetonitrile–HEPES buffer (2:8 pH 7.4) solution.

combined. After 1 day, 6 mL of diethyl ether was slowly added to the solution and dark blue block-type crystals formed in a few days. Anal. Calcd. for $C_{50}H_{45}Cu_2N_9O_7$ (1011.06 g/mol): C, 59.40; H, 4.49; Cu, 12.57; N, 12.47. Found: C, 59.40; H, 4.49; Cu, 12.57; N, 12.47.

4.4. UV–vis and fluorescence of metal ions

Stock solutions (0.02 M) of the nitrate salts of Na^+, K^+, Mg^{2+}, Ca^{2+}, Cr^{3+}, Mn^{2+}, Fe^{3+}, Co^{2+}, Ni^{2+}, Cu^{2+}, Zn^{2+}, Cd^{2+}, Hg^{2+}, Pb^{2+}, Al^{3+}, Ga^{3+} and In^{3+} in acetonitrile were prepared. Solutions of receptor (10 or 20 μM) were also prepared in buffer–acetonitrile (10 mM HEPES, pH 7.4, 1:1 or 2:8, v/v). 1.5 or 3 μL of stock solutions (0.02 M) of the metal nitrate salts were transferred to 3 mL of a solution of receptor (10 or 20 μM). The absorption and fluorescence after excited at 356 nm of the solutions were tested.

4.5. Naked-eye and UV–vis detection of receptor with Co^{2+} and Cu^{2+}

For the detection by naked-eye, stock solutions (0.02 M) of the nitrate salts of Na^+, K^+, Mg^{2+}, Ca^{2+}, Cr^{3+}, Mn^{2+}, Fe^{3+}, Co^{2+}, Ni^{2+}, Cu^{2+}, Zn^{2+}, Cd^{2+}, Hg^{2+}, Pb^{2+}, Al^{3+}, Ga^{3+} and In^{3+} in acetonitrile were prepared. Solutions of receptor (50 μM) were also prepared in acetonitrile–buffer solution (2:8, v/v). 7.5 μL of stock solutions (0.02 M) of the metal nitrate salts was transferred to 3 mL of the solution of receptor (50 μM). For the detection by UV–vis spectroscopy, stock solutions (0.02 M) of the nitrate salts of Na^+, K^+, Mg^{2+}, Ca^{2+}, Cr^{3+}, Mn^{2+}, Fe^{3+}, Co^{2+}, Ni^{2+}, Cu^{2+}, Zn^{2+}, Cd^{2+}, Hg^{2+}, Pb^{2+}, Al^{3+}, Ga^{3+} and In^{3+} ions in acetonitrile were prepared. Solutions of receptor (20 μM) were also prepared in acetonitrile–buffer solution (2:8, v/v). 3.0 μL of stock solutions (0.02 M) of the metal nitrate salts was transferred to 3 mL of the solution of **1** (20 μM). After shaking for a few seconds, the absorption was tested.

4.6. UV–vis titration of receptor with Co^{2+} and Cu^{2+}

Receptor was dissolved in acetonitrile–buffer solution (2:8, v/v) to make the concentration 20 μM. 1.5–24 μL of cobalt or copper nitrates (4 mM) were transferred to separate solutions of receptor (20 μM, 3 mL). After mixing for a few seconds, UV–vis spectra were taken at room temperature.

4.7. Job plot measurements of Co^{2+} and Cu^{2+}

Cobalt and copper nitrates and receptor were dissolved in acetonitrile–buffer solution (2:8, v/v), respectively, to make 80 μM solutions. Volumes of 5.0, 4.5, 4.0, 3.5, 3.0, 2.5, 2.0, 1.5, 1.0, 0.5 and 0 mL of the receptor solution were taken and transferred to vials. Volumes of 0, 0.5, 1.0, 1.5, 2.0, 2.5, 3.0, 3.5, 4.0, 4.5 and 5.0 mL of the cobalt or copper solutions were added to separate solutions of receptor. Each vial had a total volume of 5 mL. After shaking the vials for a few seconds, UV–vis spectra were taken at room temperature.

4.8. Fluorescence titration and Job plot of receptor with Zn^{2+}

Receptor was dissolved in acetonitrile–buffer solution (1:1, v/v) to make the concentration 10 μM. 0.6–9 μL of the metal nitrate (5 mM) was transferred to separate solutions of receptor (10 μM, 3 mL). After mixing for a few seconds, fluorescence spectra were taken at room temperature after excitation at 356 nm. For the Job plot, receptor and zinc nitrate were dissolved in acetonitrile–buffer solution (1:1, v/v), respectively, to make a 20 μM concentration. 5, 4.5, 4, 3.5, 3, 2.5, 2, 1.5, 1, 0.5 and 0 mL of receptor solution were taken and transferred to vials. 0, 0.5, 1, 1.5, 2, 2.5, 3, 3.5, 4, 4.5 and 5 mL of the cobalt solution were added to each solution of receptor. Each vial had a total volume of 5 mL. After shaking the vials for a few seconds, UV–vis spectra were taken at room temperature.

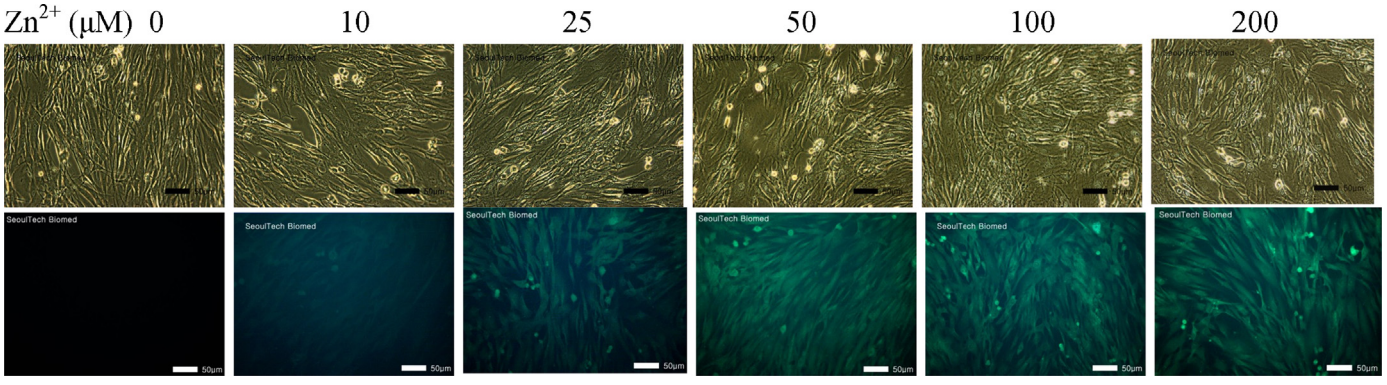

Fig. 8. Visible and fluorescent images of cells. Cells were incubated with Zn^{2+} (0–200 μM), washed with phosphate buffer, and exposed to 30 μM receptor, after which the images were taken.

4.9. UV–vis titration of receptor and Zn^{2+}

Receptor was dissolved in acetonitrile–buffer solution (1:1, v/v) to make a 40 μM solution. 2.0–36 μL of a cobalt nitrate acetonitrile solution (6 mM) were transferred to separate receptor solutions (40 μM, 3 mL). After mixing for a few seconds, UV–vis spectra were taken at room temperature.

4.10. Determination of the stability constants K and limits of detection of metal ions

The stability constants K of the receptor with Co^{2+}, Cu^{2+} and Zn^{2+} were determined by the Benesi–Hildebrand equation [23]: $1/(I-I_o) = 1/(K(I_c-I_o)[\text{metal ion}]) + 1/(I_c-I_o)$, where K is the association constant, I_o is the absorbance or fluorescence intensity of the free receptor, I is the observed absorbance or fluorescence intensity of the [receptor–metal] complex, and I_c is absorbance or fluorescence intensity of the receptor–metal complex at the saturation. In order to determine the K for Co^{2+} and Cu^{2+}, absorbance of receptor (20 μM) at 263 nm was examined upon the addition of 0–30 μM Co^{2+} or Cu^{2+} solution in buffer–acetonitrile solution (v/v = 8:2). For Zn^{2+}, fluorescence intensity of receptor (10 μM) at 520 nm was examined upon the addition of 0–10 μM Zn^{2+} solution in buffer–acetonitrile solution (v/v = 1:1).

Limits of detection where calculated by plotting concentration of metal ion versus fluorescence or absorbance. The slope of the graph was divided into three times sigma (standard deviation) to calculate the limit of detection.

4.11. NMR titration of receptor and Zn^{2+}

Four NMR tubes of receptor (0.82 mg, 0.002 mmol) dissolved in CD_3CN were prepared, and four different equivalents (0, 0.5, 1, and 2 equiv.) of zinc nitrate dissolved in CD_3CN were added separately to the receptor solutions. In aqueous environment, four NMR tubes of receptor (0.82 mg, 0.002 mmol) dissolved in a mixture of CD_3CN and D_2O (9:1, v/v) were prepared, and four different equivalents (0, 0.5, 1, and 2 equiv.) of zinc nitrate dissolved in a mixture of CD_3CN and D_2O (9:1, v/v) were added separately to the receptor solutions. After shaking for a few seconds, the ^1H NMR spectra were taken.

4.12. Methods of cell test

Human dermal fibroblast cells in low passage were cultured in FGM-2 medium (Lonza, Switzerland) supplemented with 10% fetal bovine serum, 1% penicillin/streptomycin in the in vitro incubator with 5% CO_2 at 37 °C. Cells were seeded onto a 8 well plate (SPL Lifesciences, Korea) at a density of 2×10^5 cells per well and then incubated at 37 °C for 4 h after addition of various concentrations (0–200 μM) of $Zn(NO_3)_2$ dissolved in MeCN. After washing with phosphate buffered saline (PBS) two times to remove the remaining $Zn(NO_3)_2$, the cells were incubated at room temperature with receptor (20 and 30 μM) dissolved in MeCN for 30 min. The cells were observed using a microscope (Olympus, Japan). The fluorescent images of the cells were obtained using a fluorescence microscope (Leica DMLB, Germany) at the excitation wavelength of 425 nm.

4.13. X-ray crystallography

A dark blue block-type crystal, approximate dimensions 0.36 mm × 0.16 mm × 0.16 mm, was used for the X-ray crystallographic analysis. The diffraction data for the compound was collected on a Bruker SMART APEX diffractometer equipped with a monochromator in the Mo Ka (k = 0.71073 Å) incident beam. The crystal was mounted on a silicone loop and collected data at 170 K. The CCD data were integrated and scaled using the Bruker-SAINT software package, and the structure was solved and refined using SHEXTL V6.12. All hydrogen atoms except imine hydrogen atom were located in the calculated positions. The crystallographic data, bond lengths and angles are given in supporting information. Structural information was deposited at the Cambridge Crystallographic Data Center (CCDC 1005200).

Supplementary material

Crystallographic data in CIF format. The CIF deposition number is CCDC 1005200. These files contain all the crystallographic details of this publication and are available free of charge at www.ccdc.cam.ac.uk/conts/retrieving.html or can be ordered from the following address: Cambridge Crystallographic Data Centre, 12 Union Road, GB-Cambridge CB21EZ. Fax: +44 1223 336 033; or deposit@ccdc.cam.ac.uk

Acknowledgements

Financial support from Converging Research Center Program through the National Research Foundation of Korea (NRF) funded by the Ministry of Education, Science and Technology (2012001725 and 2012008875), and Brigham Young University is gratefully acknowledged.

Appendix A. Supplementary data

Supplementary data associated with this article can be found, in the online version, at http://dx.doi.org/10.1016/j.snb.2015.02.094.

References

[1] (a) N.C. Lim, H.C. Freake, C. Brückner, Illuminating zinc in biological systems, Chem. Eur. J. 11 (2005) 38–49;
(b) Z. Dai, J.W. Canary, Tailoring tripodal ligands for zinc sensing, New J. Chem. 31 (2007) 1708–1718;
(c) E.L. Que, W. Eomaille, C.J. Chang, Metals in neurobiology: probing their chemistry and biology with molecular imaging, Chem. Rev. 108 (2008) 1517–1549;
(d) E. Tomat, S.J. Lippard, Imaging mobile zinc in biology, Curr. Opin. Chem. Biol. 14 (2010) 225–230;
(e) C. Zhang, Z. Liu, Y. Li, W. He, X. Gao, Z. Guo, In vitro and in vivo imaging application of a 1,8-naphthalimide-derived Zn^{2+} fluorescent sensor with nuclear envelope penetrability, Chem. Commun. 49 (2013) 11430–11432;
(f) Z. Liu, C. Zhang, Y. Chen, F. Qian, Y. Bai, W. He, Z. Guo, *In vivo* ratiometric Zn^{2+} imaging in zebrafish larvae using a new visible light excitable fluorescent sensor, Chem. Commun. 50 (2014) 1253–1255.
[2] (a) L.E. McQuade, S.J. Lippard, Cell-trappable quinoline-derivatized fluoresceins for selective and reversible biological Zn(II) detection, Inorg. Chem. 49 (2010) 9535–9545;
(b) B.A. Smith, W.J. Akers, W.M. Leevy, A.J. Lampkins, S. Xiao, W. Wolter, M.A. Suckow, S. Achilefu, B.D. Smith, Optical imaging of mammary and prostate tumors in living animals using a synthetic near infrared zinc(II)-dipicolylamine probe for anionic cell surfaces, J. Am. Chem. Soc. 132 (2010) 67–69;
(c) Z. Xu, K.-H. Baek, H.N. Kim, J. Cui, X. Qian, D.R. Spring, I. Shin, J. Yoon, Zn^{2+}-triggered amide tautomerization produces a highly Zn^{2+}-selective, cell-permeable, and ratiometric fluorescent sensor, J. Am. Chem. Soc. 132 (2010) 601–610;
(d) E.M. Nolan, S.J. Lippard, Small-molecule fluorescent sensors for investigating zinc metalloneurochemistry, Acc. Chem. Res. 42 (2009) 193–203;
(e) Y. Mei, C.J. Frederickson, L.J. Giblin, J.H. Weiss, Y. Medvedeva, P.A. Bentley, Sensitive and selective detection of zinc ions in neuronal vesicles using PYDPY1, a simple turn-on dipyrrin, Chem. Commun. 47 (2011) 7107–7109.
[3] (a) C.-Y. Tsai, Y.-W. Lin, A highly selective and sensitive fluorescence assay for determination of copper(II) and cobalt(II) ions in environmental water and toner samples, Analyst 138 (2013) 1232–1238;
(b) H.Y. Au-Yeung, E.J. New, C.J. Chang, A selective reaction-based fluorescent probe for detecting cobalt in living cells, Chem. Commun. 48 (2012) 5268–5270;
(c) D. Maity, V. Kumar, T. Govindaraju, Reactive probes for ratiometric detection of Co^{2+} and Cu^{+} based on excited-state intramolecular proton transfer mechanism, Org. Lett. 14 (2012) 6008–6011;
(d) I. Grabchev, D. Staneva, S. Dumas, J.-M. Chovelon, Metal ions and protons sensing properties of new fluorescent 4-N-methylpiperazine-1,8-naphthalimide terminated poly(propyleneamine) dendrimer, J. Mol. Struct. 27 (2011) 16–21.

[4] (a) S. Sombatsri, J. Wittayakun, K. Sanai, K. Kajsanthia, S. Prayoonpokarach, An optical sensing film for the determination of Co(II) based on disodium-1-nitroso-2-naphthol-3,6-disulfonate immobilized in chitosan film, Sens. Actuators B: Chem. 166–167 (2012) 772–776;
(b) Y. Leng, F. Zhang, Y. Zhang, X. Fu, Y. Weng, L. Chen, A. Wu, A rapid and sensitive colorimetric assay method for Co^{2+} based on the modified Au nanoparticles (NPs): understanding the involved interactions from experiments and simulations, Talanta 94 (2012) 271–277;
(c) A.H. Gore, D.B. Gunjal, M.R. Kokate, V. Sudarsan, P.V. Anbhule, S.R. Patil, G.B. Kolekar, Highly selective and sensitive recognition of cobalt(II) ions directly in aqueous solution using carboxyl-functionalized CdS quantum dots as a naked eye colorimetric probe: applications to environmental analysis, ACS Appl. Mater. Interfaces 4 (2012) 5217–5226;
(d) D. Maity, T. Govindaraju, Highly selective colorimetric chemosensor for Co^{2+}, Inorg. Chem. 50 (2011) 11282–11284;
(e) S.J. Zhen, F.L. Guo, L.Q. Chen, Y.F. Li, Q. Zhang, C.Z. Huang, Visual detection of cobalt(II) ion in vitro and tissue with a new type of leaf-like molecular microcrystal, Chem. Commun. 47 (2011) 2562–2564;
(f) Y. Yao, D. Tian, H. Li, Cooperative binding of bifunctionalized and click-synthesized silver nanoparticles for colorimetric Co^{2+} sensing, ACS Appl. Mater. Interfaces 2 (2010) 684–690.
[5] (a) X. Lou, Y. Zhang, Q. Li, J. Qin, Z. Li, A highly specific rhodamine-based colorimetric probe for hypochlorites: a new sensing strategy and real application in tap water, Chem. Commun. 47 (2011) 3189–3191;
(b) L. Tang, F. Li, M. Liu, R. Nandhkumar, Single sensor for two metal ions: colorimetric recognition of Cu^{2+} and fluorescent recognition of Hg^{2+}, Spectrochim. Acta A 78 (2011) 1168–1172;
(c) N. Narayanaswamy, T. Govindaraju, Aldazine-based colorimetric sensors for Cu^{2+} and Fe^{3+}, Sens. Actuators B: Chem. 161 (2012) 304–310.
[6] J.Y. Noh, G.J. Park, Y.J. Na, H.Y. Jo, S.A. Lee, C. Kim, A colorimetric "naked-eye" Cu(II) chemosensor and pH indicator in 100% aqueous solution, Dalton Trans. 43 (2014) 5652–5656.
[7] K.B. Kim, H. Kim, E.J. Song, S. Kim, I. Noh, C. Kim, A cap-type Schiff base acting as a fluorescence sensor for zinc(II) and a colorimetric sensor for iron(II), copper(II), and zinc(II) in aqueous media, Dalton Trans. 42 (2013) 16569–16577.
[8] (a) X. Zhang, M. Kang, H.-A. Choi, J.Y. Jung, K.M.K. Swamy, S. Kim, D. Kim, J. Kim, C. Lee, J. Yoon, Organic radical-induced Cu^{2+} selective sensing based on thiazolothiazole derivatives, Sens. Actuators B: Chem. 192 (2014) 691–696;
(b) Q. Lin, P. Chen, J. Liu, Y.-P. Fu, Y.-M. Zhang, T.-B. Wei, Colorimetric chemosensor and test kit for detection copper (II) cations in aqueous solution with specific selectivity and high sensitivity, Dyes Pigments 98 (2013) 100–105;
(c) D. Maity, A.K. Manna, D. Karthigeyan, T.K. Kundu, S.K. Pati, T. Govindaraju, Visible–near-infrared and fluorescent copper sensors based on julolidine conjugates: selective detection and fluorescence imaging in living cells, Chem. Eur. J. 17 (2011) 11152–11161;
(d) Q. Xu, K.M. Lee, F. Wang, J. Yoon, Visual detection of copper ions based on azide- and alkyne-functionalized polydiacetylene vesicles, J. Mater. Chem. 21 (2011) 15214–15217.
[9] H.N. Kim, W.X. Ren, J.S. Kim, J. Yoon, Fluorescent and colorimetric sensors for detection of lead, cadmium, and mercury ions, Chem. Soc. Rev. 41 (2012) 3210–3244.
[10] J.Y. Jung, S.J. Han, J. Chun, C. Lee, J. Yoon, New thiazolothiazole derivatives as fluorescent chemosensors for Cr^{3+} and Al^{3+}, Dyes Pigments 94 (2012) 423–426.
[11] J. Mao, L. Wang, W. Dou, X. Tang, Y. Yan, W. Liu, Tuning the selectivity of two chemosensors to Fe(III) and Cr(III), Org. Lett. 9 (2007) 4567–4570.
[12] N. Singh, N. Kaur, C.N. Choitir, J.F. Callan, A dual detecting polymeric sensor: chromogenic naked eye detection of silver and ratiometric fluorescent detection of manganese, Tetrahedron Lett. 50 (2009) 4201–4204.
[13] (a) S. Sen, S. Sarkar, b. Chattopadhyay, A. Moirangthaem, A. Basu, K. Dhara, P. Chattopadhyay, A dual detecting polymeric sensor: chromogenic naked eye detection of silver and ratiometric fluorescent detection of manganese, Analyst 137 (2012) 3335–3342;
(b) Q. Mei, C. Jiang, G. Guan, K. Zhang, B. Liu, R. Liu, Z. Zhang, Fluorescent graphene oxide logic gates for discrimination of iron (3+) and iron (2+) in living cells by imaging, Chem. Commun. 48 (2012) 7468–7470.
[14] D.Y. Lee, N. Singh, D.O. Jang, Ratiometric and simultaneous estimation of Fe^{3+} and Cu^{2+} ions: 1,3,5-substituted triethylbenzene derivatives coupled with benzimidazole, Tetrahedron Lett. 52 (2011) 3886–3890.
[15] S. Wang, G. Men, L. Zhao, Q. Hou, S. Jiang, Binaphthyl-derived salicylidene Schiff base for dual-channel sensing of Cu, Zn cations and integrated molecular logic gates, Sens. Actuators B: Chem. 145 (2010) 826–831.
[16] (a) H.Y. Lee, K.M.K. Swamy, J.Y. Jung, G. Kim, J. Yoon, Rhodamine hydrazine derivatives based selective fluorescent and colorimetric chemodosimeters for Hg^{2+} and selective colorimetric chemosensor for Cu^{2+}, Sens. Actuators B: Chem. 182 (2013) 530–537;
(b) L. Tang, F. Li, M. Liu, R. Nandhakumar, Single sensor for two metal ions: colorimetric recognition of Cu^{2+} and fluorescent recognition of Hg^{2+}, Spectrochim. Acta A 78 (2011) 1168–1172.
[17] D. Maity, T. Govindaraju, A differentially selective sensor with fluorescence turn-on response to Zn^{2+} and dual-mode ratiometric response to Al^{3+} in aqueous media, Chem. Commun. 48 (2012) 1039–1041.
[18] E.J. Song, J. Kang, G.R. You, G.J. Park, Y. Kim, S.J. Kim, C. Kim, R.G. Harrison, A single molecule that acts as a fluorescence sensor for zinc and cadmium and a colorimetric sensor for cobalt, Dalton Trans. 42 (2013) 15514–15520.
[19] A. Trösch, H. Vahrenkamp, Zinc complexes of tripodal N_3O ligands, Eur. J. Inorg. Chem. 6 (1998) 827–832.
[20] (a) Y. Zhang, X. Guo, L. Jia, S. Zu, Z. Xu, L. Zheng, X. Qian, Substituent-dependent fluorescent sensors for zinc ions based on carboxamidoquinoline, Dalton Trans. 41 (2012) 11776–11782;
(b) Y. Zhang, X. Guo, W. Si, L. Jia, X. Qian, Ratiometric and water-soluble fluorescent zinc sensor of carboxamidoquinoline with an alkoxyethylamino chain as receptor, Org. Lett. 10 (2008) 473–476;
(c) X. Zhou, B. Yu, Y. Guo, X. Tang, H. Zhang, W. Liu, Both visual and fluorescent sensor for Zn^{2+} based on quinoline platform, Inorg. Chem. 49 (2010) 4002–4007;
(d) X. Zhou, P. Li, Z. Shi, X. Tang, C. Chen, W. Liu, A highly selective fluorescent sensor for distinguishing cadmium from zinc ions based on a quinoline platform, Inorg. Chem. 51 (2012) 9226–9231;
(e) R.-M. Wang, S.-B. Huang, N. Zhao, Z.-N. Chen, A new Zn^{2+} chemosensor based on functionalized 8-hydroxylquinoline, Inorg. Chem. Commun. 13 (2010) 1432–1434;
(f) C. Núñez, R. Bastida, A. Macías, E. Bértolo, L. Fernandes, J.L. Capelo, C. Lodeiro, Synthesis, characterization, and fluorescence behavior of four novel macrocyclic emissive ligands containing a flexible 8-hydroxyquinoline unit, Tetrahedron 65 (2009) 6179–6188;
(g) M. Mameli, M.C. Aragoni, M. Arca, M. Atzori, A. Bencini, C. Bazzicalupi, A.J. Blake, C. Caltagirone, F.A. Devillanova, A. Garau, M.B. Hursthouse, F. Isaia, V. Lippolis, B. Valtancoli, Synthesis and coordination properties of quinoline pendant arm derivatives of [9]$aneN_3$ and [9]$aneN_2S$ as fluorescent zinc sensors, Inorg. Chem. 48 (2009) 9236–9249;
(h) J. Jiang, T. Xiaoliang, L. Yang, W. Dou, W. Liu, R. Fang, W. Liu, An efficient sensor for Zn^{2+} and Cu^{2+} based on different binding modes, Dalton Trans. 40 (2011) 6367–6370;
(i) I. Ravikumar, P. Ghosh, Zinc(II) and PPi selective fluorescence OFF–ON–OFF functionality of a chemosensor in physiological conditions, Inorg. Chem. 50 (2011) 4229–4231;
(j) C. Zhao, Y. Zhang, P. Feng, J. Cao, Development of a borondipyrromethene-based Zn^{2+} fluorescent probe: solvent effects on modulation sensing ability, Dalton Trans. 41 (2012) 831–838;
(k) E.M. Nolan, J. Jaworski, K.-I. Okamoto, Y. Hayashi, M. Sheng, S.J. Lippard, QZ1 and QZ2: rapid, reversible quinoline-derivatized fluoresceins for sensing biological Zn(II), J. Am. Chem. Soc. 127 (2005) 16812–16823;
(l) J.-F. Zhu, H. Yuan, W.-H. Chan, A.W.M. Lee, A FRET fluorescent chemosensor SPAQ for Zn^{2+} based on a dyad bearing spiropyran and 8-aminoquinoline unit, Tetrahedron Lett. 51 (2010) 3550–3554.
[21] H.A. Benesi, J.H. Hildebrand, A spectrophotometric investigation of the interaction of iodine with aromatic hydrocarbons, J. Am. Chem. Soc. 71 (1949) 2703–2707.
[22] H.G. Lee, J.H. Lee, S.P. Jang, I.H. Hwang, S.-J. Kim, J. Kim, C. Kim, R.G. Harrison, Zinc selective chemosensors based on the flexible dipicolylamine and quinoline, Inorg. Chim. Acta 394 (2013) 542–551.
[23] J.H. Kim, I.H. Hwang, S.P. Jang, J. Kang, S. Kim, I. Noh, Y. Kim, C. Kim, R.G. Harrison, Zinc sensors with lower binding affinities for cellular imaging, Dalton Trans. 42 (2013) 5500–5507.

Biographies

Eun Joo Song received the BS degree in 2012 at Seoul National University of Science and Technology. She is currently a master's degree student at Seoul National University of Science and Technology. Her research interest includes chemical sensors, synthesis of catalyst and inorganic medicine.

Gyeong Jin Park earned the BS degree in 2013 at Seoul National University of Science and Technology. She is currently a master's degree student at Seoul National University of Science and Technology. Her scientific interest includes chemical sensors, synthesis of catalyst and inorganic medicine.

Jae Jun Lee earned the BS degree in 2014 at Seoul National University of Science and Technology. He is currently a master's degree student at Seoul National University of Science and Technology. His scientific interest includes, molecular modeling, chemical sensors, and synthesis of catalyst.

Suyeon Lee received the BS degree in 2012 at Seoul National University of Science and Technology. She is currently a master's degree student at Seoul National University of Science and Technology. Her research interests focus on tissue engineering.

Dr. Insup Noh is currently a Professor at Seoul National University of Science and Technology. He received the Ph.D. degree in 1997 at University of Texas at Austin, USA. He is now interested in development of polymeric biomaterials for local delivery of bioactive agents and tissue engineering of bone, cartilage and nerve.

Dr. Youngmee Kim is currently a research professor at Ewha Womans University. She received the Ph.D. degree in 1993 at Texas A&M University, USA. She is interested in inorganic chemistry and her research interests focus on syntheses and applications of MOFs (Metal-Organic Frameworks).

Dr. Sung-Jin Kim is currently a professor at Ewha Womans University. She received the Ph.D. degree in 1989 at Iowa State University, USA. She is interested in materials chemistry, nanochemistry, solid-state chemistry, and inorganic chemistry. Her research interests focus on thermoelectric materials and solar cell.

Dr. Cheal Kim is currently a professor at Seoul National University of Science and Technology. He received the Ph.D. degree in 1993 at University of California, San Diego, USA. He is now interested in the development of chemical sensors, reactivity study of the transition metal complexes, DNA cleavage by their metal complexes, and MOF.

Dr. Roger G. Harrison is currently a professor at Brigham Young University. He received a Ph.D. degree in 1993 at the University of Utah, USA. His current research interests include separation materials for ion chromatography, host–guest complexes, chemical sensors, and nanomaterials.